Catalytic activity toward oxygen reduction of transition metal porphyrins covalently linked to single-walled carbon nanotubes: A density functional study

Walter Orellana

Departamento de Ciencias Físicas, Universidad Andres Bello, Avenida República 220, 837-0134, Santiago, Chile

(Received 2 August 2011; revised manuscript received 15 September 2011; published 7 October 2011)

The interaction of molecular oxygen with the metal center of transition metal porphyrins (MP, with M = Mn, Fe, Co, and Ni) covalently linked to single-walled carbon nanotubes (CNTs) are addressed by density functional theory calculations. Two geometries for the CNT sidewall functionalization with porphyrin radicals are proposed, considering sp^2 and sp^3 chemical bonds. By computing the stability and electronic properties of the CNT-MP complexes, and the interaction of the O_2 molecule with the metal center, we investigate their catalytic activity toward the oxygen reduction reaction (ORR). According to our results, CNT-MnP, CNT-CoP, and CNT-FeP linked by sp^2 covalent bonds are highly stable, preserving the CNT metallic character. We also find a significant O–O bond weakening after the oxygen adsorption on the porphyrin metal center, showing favorable conditions toward ORR. These results support experimental evidences of ORR activity in CNT-based transition metal-N_4 centers.

DOI: 10.1103/PhysRevB.84.155405 PACS number(s): 73.22.−f, 68.43.Bc, 68.43.Hn

I. INTRODUCTION

Covalent functionalization of carbon nanotubes (CNTs) with transition metal macrocycles (e.g., porphyrins and phthalocyanine) are thought to be a promising class of materials for the oxygen reduction reaction (ORR) with the potential to substitute platinum in polymer electrolyte membrane (PEM) fuel cells.[1,2] Indeed, cobalt porphyrins covalently linked to multiwalled carbon nanotubes have shown superior catalytic performance for ORR at room temperature.[3] This performance is attributed to the mechanical strength and electrical conductivity of the functionalized-CNT electrodes, providing the necessary stability and charge for the metal macrocycles to work in the corrosive environment of PEM fuel cells. Similar results have been found in other carbon-supported catalysts containing the same active sites of metal macrocycles (e.g., Fe-N_4 and Co-N_4).[4–7] However, little is known about the structural and electronic properties of carbon-supported transition metal-N_4 centers interacting with the oxygen molecule to have clear picture of the reduction property reported.

Recently, Shi and Zhang[8] have addressed the relationship between experimental oxygen-reduction catalytic activity of different transition metal macrocycles and some calculated equilibrium properties. For the available experimental data they showed that the catalytic activity of transition metal macrocycles toward ORR is directly related to the ionization potential and the O_2 heat of adsorption on the macrocyclic metal center. That work demonstrated that higher ionization potentials and larger O_2 binding energies can be associated with a better catalytic activity, which has proved to be consistent with well-established redox mechanisms.[9,10] Following this idea, we investigate the catalytic activity of transition metal porphyrins (MP, with M = Mn, Fe, Co, and Ni) covalently linked to metallic CNTs, hereafter called the CNT-MP complex. By computing binding energies and the stretching frequency of O_2 adsorbed on the metal center of CNT-MP we study the initial step for the oxygen dissociation. The O_2 adsorption on the catalyst active site is thought to be the most important intermediate for the ORR activity in several systems.[7,11,12] This reaction originates in the ability of the catalyst to donate an electron to the antibonding molecular orbital, weakening the O–O bond, and eventually inducing the dissociation. Therefore the O–O stretching frequency of the adsorbed molecule can give us a direct parameter to compare ORR activity for different CNT-supported metal porphyrins. We also investigate the electronic band structure of these complexes to clarify the electron-donating properties of the CNT-MP complexes and the role of the metal atom.

II. THEORETICAL APPROACH

By using the SIESTA code,[13] we perform first-principles electronic-structure calculations based on the density functional theory, within the generalized gradient approximation, to the exchange and correlation functional (GGA-PBE).[14] A basis set of localized atomic orbitals (double-ζ plus polarization functions) and norm-conserving pseudopotentials were employed. The partial core correction and relativistic effects for transition metal pseudopotentials were included. The transition metal porphyrins (MPs) are covalently linked to a metallic (8,8) CNT of 11 Å diameter. The CNT-MP complexes are described within a cubic supercell of side $12a_0$, where $a_0 = 2.49$ Å is the length of the CNT unit cells. Thus the minimum separation between CNT-MP images is fixed to be about 8 Å, which proved to be enough to avoid interactions between them. The Brillouin zone sampling was performed with the Γ point for the geometry optimization and with a $2 \times 2 \times 2$ k-point mesh for the electronic properties. The CNT-MP complexes are fully relaxed until the force on each atom is less than 0.05 eV/Å. Convergence tests considering a smaller force threshold of 0.01 eV/Å show negligible changes in the equilibrium geometry. Binding energies are calculated by the energy difference between adsorbed and separated constituents, considering corrections due to the basis set superposition error.

In a previous work we investigated different mechanisms to attach an iron porphyrin (FeP) on the surface of metallic and semiconducting CNTs, including physisorption and chemisorption.[15] Those results suggest that covalent

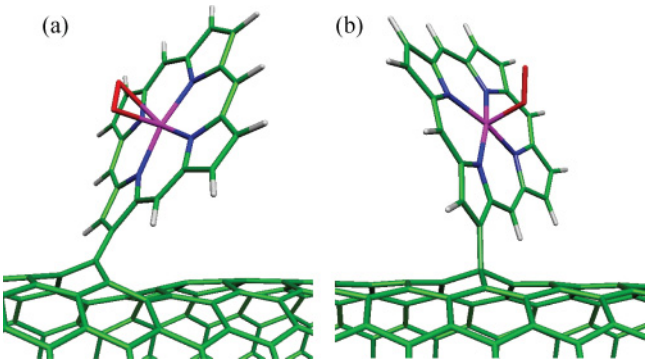

FIG. 1. (Color online) Stable geometries of O_2 adsorbed on the metal center of porphyrins anchored to a carbon nanotube (CNT-MP). (a) O_2 in the sideon geometry and CNT-MP in the sp^2 bonding structure. (b) O_2 in the endon geometry and CNT-MP in the sp^3 bonding structure.

functionalization of metallic CNTs with FeP would meet the conditions to explain the experimentally reported ORR activity of carbon-supported Fe-N_4 systems.[4,6] This conclusion was based on the metallic character and stability observed in the CNT-FeP complex which would ensure the charge transfer to the macrocycle. Figure 1 shows two plausible geometries for the CNT covalent functionalization with metal porphyrins as considered in the present work. In one case an sp^2 bonding is formed when an undercoordinated C atom of a metal porphyrin radical (without an H atom) finds a twofold-coordinated C atom in the CNT, for instance, those at the CNT ends or in CNTs containing a single vacancy, as shown in Fig. 1(a). Here the radical binding energy is found to be 4.11 eV. In the other case, the undercoordinated C atom of the metal porphyrin radical binds to a C atom of a pristine CNT, forming an sp^3 bonding structure, as shown in Fig. 1(b). Here the radical has a binding energy of 1.13 eV, considerably weaker than the sp^2 attachment.

III. RESULTS AND DISCUSSION

A. Electronic properties of carbon nanotube-metal porphyrin complexes

As a first step, the geometry and electronic properties of the isolated metal porphyrins are investigated. Table I summarizes average bond distances between the metal center and the nitrogen atoms (d_{M-N}), as well as between nitrogens and carbons (d_{N-C}). The first ionization energy (IE) and the spin magnetic moment (m) are also calculated. According to the magnetic moments, we observe that from NiP to MnP the number of parallel-spin $3d$ electrons of the metal center increases from zero to three, lengthening the M–N bond distance due to the increase in the exchange interaction. Consequently, the calculated ionization energy decreases from 6.8 to 5.4 eV. These results agree well with other calculations,[8,16] as well as with x-ray diffraction experiments,[17,18] ensuring a good description for the metal porphyrins.

TABLE I. Bond distance (d), first ionization energy (IE), and magnetic moment (m) of the transition metal porphyrins.

Molecule	d_{M-N} (Å)	d_{N-C} (Å)	IE (eV)	m (μ_B)
MnP	2.017	1.398	5.39	3.0
FeP	1.990	1.397	5.98	2.0
CoP	1.986	1.394	6.72	1.0
NiP	1.968	1.395	6.76	0.0

TABLE II. Bond distance (d), work function (WF), and spin magnetic moment (m) of transition metal porphyrins covalently linked to the CNT surface through sp^2 and sp^3 bonding.

Complex	d_{M-N} (Å)	d_{N-C} (Å)	WF (eV)	m (μ_B)
CNT-MnP (sp^2)	2.013	1.397	4.27	3.4
CNT-FeP (sp^2)	1.991	1.398	4.32	2.2
CNT-CoP (sp^2)	1.983	1.394	4.36	1.0
CNT-NiP (sp^2)	1.962	1.394	4.32	0.0
CNT-MnP (sp^3)	2.004	1.396	4.25	3.4
CNT-FeP (sp^3)	1.982	1.396	4.33	2.2
CNT-CoP (sp^3)	1.976	1.393	4.40	1.0
CNT-NiP (sp^3)	1.958	1.393	4.40	0.0

Next we investigate the properties of metal porphyrins attached on the CNT surface. Table II summarizes our results for average bond distances, spin magnetic moment, and work function for the CNT-MP complexes in the sp^2 and sp^3 bonding structures. The work function is calculated by takeing the difference between the Fermi energy and the vacuum reference energy. We verify that the metal porphyrin geometry and the magnetic moment remains almost unchanged when the porphyrin is attached to the CNT. We also note a small polarization on the nanotube induced by the MP metal center, which changes slightly the total magnetic moment of the complexes. First ionization energy and work functions were calculated in order to compare the energy required to remove an electron from the isolated MP and from the CNT-MP complex, respectively. Our results show that the CNT-MP work functions keep almost constant, around 4.3 eV, which is a typical value observed in carbon nanotubes,[19,20] contrasting with the MP ionization energies which vary in a range of 5.4–6.8 eV. Thus it is clear that it costs less energy to remove an electron from CNT-MP than from isolated MPs, mainly due to the metallic character of the complexes. In transition metal macrocycles, the ORR activity has been related to the ionization potential, where larger ionization potentials are associated with higher ORR activity.[8] In CNT-MP complexes this is not clear, because the work function, the equivalent to the molecular ionization potential, has a relatively small variation with respect to the porphyrin metal.

Figure 2 shows the spin-resolved band structure of the CNT-MP complexes in the sp^2 and sp^3 bonding geometries. We see that the MP attachment alters significantly the CNT band structure, breaking its symmetry and showing a strong hybridization with the MP molecular orbitals. We also note that the two kinds of MP attachments, the stronger sp^2 and the weaker sp^3, change drastically the functionalized-CNT electronic properties, which could be key for the ORR catalytic activity. Figures 2(a)–2(d) show the CNT-MP band structures for the sp^2 bonding geometry. We see that all complexes

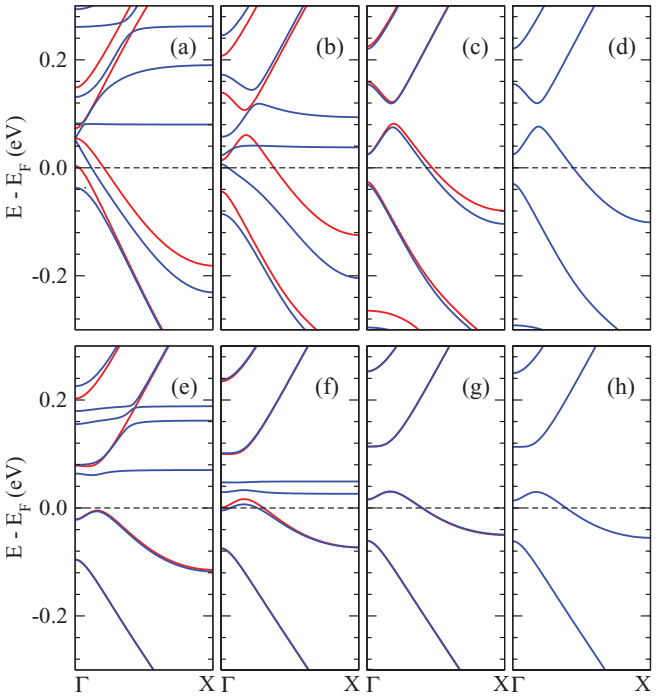

FIG. 2. (Color online) Spin-resolved band structure of carbon nanotube-metal porphyrin complexes: (a)–(d) in the sp^2 structure for CNT-MnP, CNT-FeP, CNT-CoP, and CNT-NiP, (e)–(h) in the sp^3 structure for CNT-MnP, CNT-FeP, CNT-CoP, and CNT-NiP. Blue (red) curves represent majority (minority) spin subbands.

show a metallic character, where CNT-MnP and CNT-FeP [Figs. 2(a) and 2(b)] exhibit a large exchange splitting between majority and minority spin subbands. Considering that the charge transfer from the complex metal center to the adsorbed O_2 is the key mechanism for the oxygen reduction, our results suggest that all the complexes in the sp^2 bonding geometry would have favorable conditions toward the ORR. In the sp^3 bonding geometry [Figs. 2(e)–2(h)], the influence of the metal center appears to be more drastic. In CNT-MnP we find an energy gap that turns the functionalized CNT into a semiconductor [Fig. 2(e)]. CNT-FeP is closer to a semimetal with a small density of states at the Fermi level [Fig. 2(f)], while CNT-CoP and CNT-NiP preserve their metallic properties but with increasing energy gaps. Therefore in the sp^3 bonding geometry only CNT-MnP would have limited catalytic activity due to the semiconducting character. The charge density associated with the states that cross the Fermi level in the metallic complexes are concentrated mostly at the porphyrin metal atom. This indicates that the catalytic active site is the metal atom, considering that any electron-transfer process must involve the states at the Fermi level.

B. Dioxygen interaction with metal porphyrins

We now present our results for the interaction of the O_2 with the porphyrin metal center. Two stable geometries are typically found for the MP:O_2 adduct: one with both O atoms bonded to the metal center, parallel to the porphyrin plane, known as *sideon* [Fig. 1(a)], and the other with an O atom bonded to the metal center, normal to the porphyrin plane, known as *endon* [Fig. 2(a)]. For MnP:O_2 both geometries sideon and endon are found, with the former being the most stable by 0.12 eV. CoP:O_2 also exhibits both geometries, with endon being the most stable by 0.23 eV. For FeP:O_2 and NiP:O_2 only the endon geometry is found.

TABLE III. Binding energy (E_b), bond length (d), stretching frequency (ν), and magnetic moment (m) for O_2 adsorbed on the MP metal center in the equilibrium geometry. Results for gas phase O_2 are also included for comparison.

Adduct	E_b (eV)	d_{O-O} (Å)	d_{M-O} (Å)	ν_{O-O} (cm^{-1})	m (μ_B)
O_2	–	1.241	–	1574	2.0
MnP:O_2 (sideon)	0.40	1.311	2.265	1262	5.0
FeP:O_2 (endon)	0.41	1.277	1.839	1343	0.0
CoP:O_2 (endon)	0.32	1.272	1.910	1390	1.0
NiP:O_2 (endon)	0.05	1.267	1.226	1437	2.0

Table III lists our results for the binding energy, bond length, stretching frequency, and magnetic moment for the MP:O_2 adducts in the equilibrium geometry. The frequencies are calculated considering small dislocations of the O_2 bond distance around its equilibrium position (less than 3%). O_2 bond length and stretching frequency in the gas phase are calculated to be 1.24 Å and 1574 cm^{-1} (experimental values are 1.21 Å and 1580 cm^{-1}). We note that the GGA-PBE prediction for O_2 stretching frequency is in close agreement with experimental data, which is partly fortuitous since DFT-GGA calculations are affected by cancellation errors. However, we can use these frequencies as a parameter to measure the O_2 bond strength after the interaction with the porphyrin's metal center.

MnP:O_2 in the equilibrium geometry (sideon) is one of most stable adducts, with a binding energy of 0.40 eV. The O_2 bond distance (1.31 Å) and stretching frequency (1262 cm^{-1}) indicate that the adsorbed molecule is notably weakened after the interaction with the porphyrin metal center. MnP:O_2 is also stable in the endon geometry, with O_2 binding energy and stretching frequency of 0.27 eV and 1312 cm^{-1}, respectively, indicating a stronger O–O bond for the metastability. In the sideon geometry this adduct shows a high-spin configuration with magnetic moment of 5 μ_B, while in the less stable endon it has a low-spin configuration (3 μ_B). The CoP:O_2 adduct is also found in endon and sideon geometries. In the most stable (endon) the O_2 binding energy and stretching frequency are 0.32 eV and 1390 cm^{-1}, while in less stable (sideon) they are 0.09 eV and 1441 cm^{-1}, respectively, again indicating a stronger O–O bond for the metastability. Concerning spin configurations, we note that the endon geometry shows low spin (1 μ_B) while sideon high spin (3 μ_B), which is the opposite of what we found in MnP:O_2.

For FeP:O_2 and NiP:O_2 only the endon geometry is found. FeP:O_2 shows an antiparallel spin coupling that results in zero magnetic moment, in agreement with previous calculations. 21 This adduct shows the highest stability, with an O_2 binding energy of 0.41 eV. However, the stretching frequency is relatively high (1343 cm^{-1}) as compared to MnP:O_2 (1262 cm^{-1}), considering that they show similar binding energies, around 0.4 eV. Finally, NiP:O_2 is found to be the weakest adduct,

with a binding energy of 0.05 eV; it also shows the highest O_2 stretching frequency (1437 cm^{-1}), indicating less favorable conditions for the O_2 dissociation. Therefore, based on the relative stretching frequency, we can order the metal porphyrin according to its effect in the oxygen bond weakening as MnP, FeP, CoP, and NiP. We also note that, in general, large adduct binding energies result in low O_2 stretching frequency, which can also be associated with the weakening of the oxygen bond.

The ORR catalytic activity of transition metal macrocycles has been related to higher ionization energies of the macrocycles and larger binding energies for the adducts. In particular, the sum of these energies was considered as a comparative parameter to determine ORR activity in metal macrocycles.[8] By evaluating this parameter we find that CoP would be the best ORR catalyst followed by NiP, FeP, and MnP. However, the O_2 stretching frequencies show that in this order the oxygen bond strength increases, which is contrary to what is expected for the ORR catalysis. According to our results, O_2 stretching frequencies and binding energies appear to be the most clear parameters suggesting better ORR activity on transition metal porphyrins.

Theoretical works on the interaction between metal porphyrins and dioxygen have been reported in the literature.[8,16,21–24] Most of these works show similar structural properties; however, important differences in the O_2 heat of adsorption and stretching frequency have been detected. The choice of the exchange-correlation functional appears to be the origin of such discrepancies. Concerning experiments, to the best of our knowledge no results on vibrational properties of metal porphyrin-O_2 adducts have been reported. However, in a close-related macrocycle, namely, tetraphenylporphyrin (TPP), experiments show O_2 stretching frequencies in MnTPP:O_2, FeTPP:O_2, and CoTPP:O_2 adducts of 983 cm^{-1} (sideon),[25] 1195 cm^{-1} (endon),[26] and 1278 cm^{-1} (endon),[27] respectively. For the same adducts we find O_2 stretching frequencies of 1193, 1315, and 1385 cm^{-1}, showing a shift to higher frequencies in the range of 107–210 cm^{-1} with respect to the experimental results. Despite the large shifts, the calculated stretching frequencies show the same trend as the experimental one, moving to higher values when the metal of the macrocycle follows the order Mn, Fe, Co. Hence we can directly associate the O_2 bond strength in the different adducts with the calculated stretching frequencies in order to compare metal porphyrin ORR activities.

C. Dioxygen interaction with carbon nanotube-metal porphyrin complexes

Table IV summarizes our results for the O_2 adsorption on the CNT-MP metal center in the two bonding structures considered (sp^2 and sp^3). For these adducts only the equilibrium geometries were considered. Comparing the results of isolated and attached porphyrins, we observe a close agreement for O_2 stretching frequencies, bond lengths, and magnetic moments. In addition, the equilibrium geometries of O_2 on the complex metal centers are also the same, suggesting that the CNT support does not change the MP:O_2 adduct properties.

The CNT-MnP complex shows the lowest stretching frequencies (1220–1260 cm^{-1}) and longest bond lengths (1.31–1.32 Å) for the O_2 adduct, which are close to those found in MnP (1262 cm^{-1} and 1.31 Å). However, the O_2 binding energy is found in the range of 0.17–0.25 eV, which is about half the value found in the isolated MnP (0.40 eV). For CNT-FeP and CNT-CoP we find similar results for the O_2 adduct, showing stretching frequencies and binding energies in the ranges of 1320–1390 cm^{-1} and 0.33–0.38 eV, respectively, which are very close to those observed in FeP and CoP. Finally, for CNT-NiP the O_2 stretching frequencies are the highest found among the complexes studied (1448–1453 cm^{-1}), while the adduct binding energy is the smallest one (0.03–0.10 eV), again following the same trend that isolated NiP. Thus we can conclude that the O_2 interaction with the porphyrin metal center is not affected by the covalent attachment on the CNT. Therefore we should expect similar ORR activity in the CNT-MP complex as that observed in the isolated metal porphyrins. We also find that higher adduct binding energies are not necessarily associated with weaker O_2 bonds in the CNT-MP:O_2 adducts.

TABLE IV. Binding energy (E_b), bond length (d), and stretching frequency (ν) of O_2 adsorbed on the metal center of CNT-MP complex in the lowest-energy configurations.

Adduct	E_b (eV)	d_{O-O} (Å)	d_{M-O} (Å)	ν_{O-O} (cm^{-1})	m_s (μ_B)
CNT-MnP:O_2 (sp^2)	0.17	1.311	2.229	1259	5.1
CNT-FeP:O_2 (sp^2)	0.33	1.276	1.842	1364	0.1
CNT-CoP:O_2 (sp^2)	0.37	1.271	1.913	1392	1.0
CNT-NiP:O_2 (sp^2)	0.03	1.266	2.257	1448	2.0
CNT-MnP:O_2 (sp^3)	0.25	1.315	2.286	1219	4.9
CNT-FeP:O_2 (sp^3)	0.37	1.273	1.853	1321	0.2
CNT-CoP:O_2 (sp^3)	0.38	1.274	1.906	1373	1.0
CNT-NiP:O_2 (sp^3)	0.10	1.264	2.262	1453	2.0

Figure 3 shows spin-density plots for O_2 adsorbed on the metal center of the CNT-MP complexes in the sp^3 attachment, the same results found in the sp^2 attachment. The shapes of the spin-density isosurfaces suggest that the porphyrin plane would be the xy plane and the metal-oxygen bond the z axis. For CNT-MnP:O_2 [Fig. 3(a)] we observe a ferromagnetic coupling between the O_2 molecule and the three unpaired electrons of MnP ($m = 3\mu_B$), probably occupying the Mn $3d_{x^2-y^2}$ and $3d_{xy}$ orbitals. For CNT-FeP:O_2 [Fig. 3(b)] we find an antiferromagnetic coupling between FeP and O_2, resulting in zero magnetic moment. The spin-density isosurfaces are equivalent to the one reported in Ref. 21. The two unpaired electrons of FeP would occupy the Fe $3d_{xz}$ or $3d_{yz}$ orbitals, according to Fig. 3(b). Similarly, for CNT-CoP:O_2 the spin configuration is antiferromagnetic with adduct magnetic moment $m = 1\mu_B$, where the CoP unpaired electron would occupy the Co $3d_{z^2}$ orbital, as shown in Fig. 3(c). In the case of CNT-NiP:O_2 there is no unpaired electron from NiP; the adduct magnetic moment ($m = 2\mu_B$) originates in the O_2 molecule, which preserves its triplet configuration when adsorbed on the metal center [Fig. 3(d)].

IV. SUMMARY AND CONCLUSION

Using *ab initio* calculations we have studied the interaction of the oxygen molecule with the metal center of transition

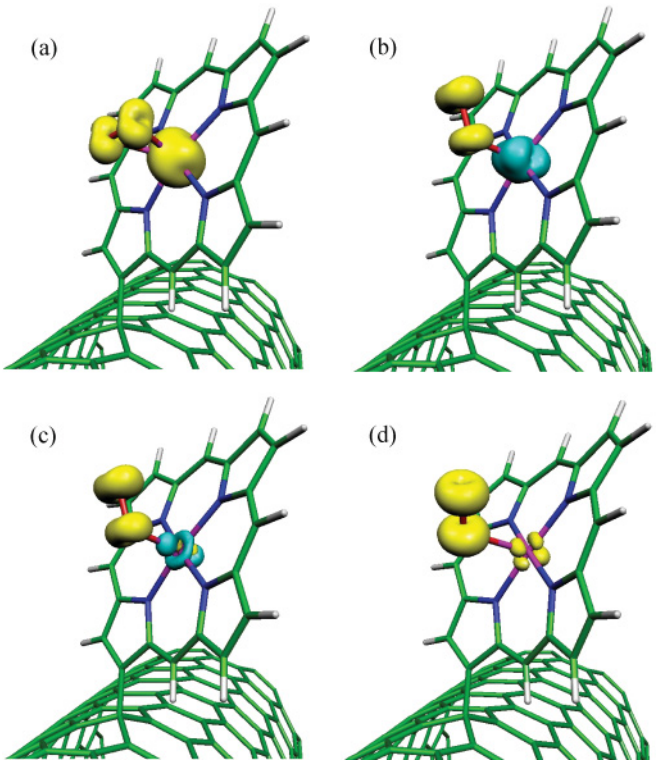

FIG. 3. (Color online) Spin-density isosurfaces for O_2 adsorbed on the porphyrin metal centers of (a) CNT-MnP, (b) CNT-FeP, (c) CNT-CoP, and (d) CNT-NiP. The isosurfaces correspond to an electronic charge of 0.02 $e/Å^3$, and different colors indicate antiparallel spin-density configurations.

metal porphyrins covalently linked to a metallic carbon nanotube. Favorable conditions toward ORR catalytic activity of the CNT-MP complexes are investigated considering three main properties: (i) the stability of the complexes, (ii) the metallic character of the functionalized CNT, and (iii) the weakness of the O_2 bond after adsorption on the porphyrin metal center. Our proposed CNT functionalization explores the formation of an sp^3 (sp^2) covalent bond between metal porphyrin radicals and pristine (defective) CNTs. Our results show that the sp^2-like functionalization is the most stable with a binding energy of 4.1 eV, considerably larger than the sp^3 (1.1 eV). Concerning the electronic properties, our results indicate different behavior depending on the porphyrin metal atom. Almost all complexes attached by sp^2 and sp^3 bonds show a metallic character. The only exception is CNT-MnP in the sp^3 bonding geometry, which opens up an energy gap of about 0.05 eV. If we consider that the CNT-MP complexes must work as cathode catalysts, high stability and good conducting properties are required. Hence the CNT functionalization with the stronger sp^2 attachments would have favorable conditions.

Next we investigated the interaction of dioxygen with the porphyrin metal center in the CNT-MP complexes. By calculating the stretching frequency of the O_2 adduct, we estimated the weakness of the O–O bond, which is the first stage toward its dissociation. According to our results, the CNT-MnP complex shows the most likely initial conditions toward ORR, exhibiting a longer and weaker O–O bond, followed by CNT-FeP and CNT-CoP. In the CNT-MnP:O_2 adduct, O_2 takes the sideon equilibrium geometry, showing a ferromagnetic coupling with the metal center, while in CNT-FeP:O_2 and CNT-CoP:O_2 it takes the endon equilibrium geometry with an antiferromagnetic coupling. For CNT-NiP:O_2, due to the absence of Ni unpaired electrons, we do not observe electronic coupling with the molecule; consequently this adduct shows the weaker interaction and the highest O_2 stretching frequency. This result suggests a close relation between the adduct spin coupling and the oxygen bond weakening. Similar results are found in freestanding metal porphyrin-O_2 adducts, suggesting that the CNT support would not affect the catalytic properties of the metal porphyrins.

In conclusion, considering stability, metallic properties, and a weaker O–O bond in the complex-O_2 adduct, our results suggest that MnP, CoP, and FeP linked to a metallic CNT with sp^2-like covalent bonds would be the best CNT-functionalized cathode catalysts for ORR. Our results support experimental evidence toward ORR activity in CNT-based metal-N_4 centers.[3–7]

ACKNOWLEDGMENTS

This work was supported by FONDECYT Grant No. 1090489 and UNAB Grant DI-02-11/R.

[1]J. P. Dodelet, in *N4-Macrocycles Metal Complexes*, edited by J. H. Zagal, F. Bedioui, and J. P. Dodelet (Springer, New York, 2006), pp. 83–147.
[2]F. Charreteur, F. Jaouen, and J. P. Dodelet, Electrochim. Acta **54**, 6622 (2009).
[3]W. Zhang, A. U. Shaikh, E. Y. Tsui, and T. M. Swager, Chem. Mater. **21**, 3234 (2009).
[4]A. L. Bouwkamp-Wijnoltz, W. Visscher, J. A. R. van Veen, E. Boellaard, A. M. van der Kraan, and S. C. Tang, J. Phys. Chem. B **106**, 12993 (2002).
[5]M. Lefèvre, J.-P. Dodelet, and P. Bertrand, J. Phys. Chem. B **109**, 16718 (2005).
[6]M. Lefèvre, E. Proietti, F. Jaouen, and J.-P. Dodelet, Science **324**, 71 (2009).
[7]D. H. Lee, W. J. Lee, W. J. Lee, S. O. Kim, and Y.-H. Kim, Phys. Rev. Lett. **106**, 175502 (2011).
[8]Z. Shi and J. Zhang, J. Phys. Chem. C **111**, 7084 (2007).
[9]J.-P. Randin, Electrochim. Acta **19**, 83 (1974).
[10]F. Beck, J. Appl. Electrochem. **7**, 239 (1977).
[11]R. Chen, H. Li, D. Chu, and G. Wang, J. Phys. Chem. C **113**, 20689 (2009).
[12]J. K. Norskov, J. Rossmeisl, A. Logadottir, L. Linqvist, J. R. Kitchin, T. Bligaard, and H. Jónsson, J. Phys. Chem. B **108**, 17886 (2004).
[13]J. M. Soler, E. Artacho, J. D. Gale, A. García, J. Junquera, P. Ordejón, and D. Sánchez-Portal, J. Phys. Condens. Matter **14**, 2745 (2002).
[14]J. P. Perdew, K. Burke, and M. Ernzerhof, Phys. Rev. Lett. **77**, 3865 (1996).

[15]I. Ruiz-Tagle and W. Orellana, Phys. Rev. B **82**, 115406 (2010).
[16]M. Tsuda, E. S. Dy, and H. Kasai, J. Chem. Phys. **122**, 244719 (2005).
[17]B. Gonzalez, J. Kouba, S. Yee, C. A. Reed, J. F. Kirner, and W. R. Scheidt, J. Am. Chem. Soc. **97**, 3247 (1975).
[18]J. P. Collman, J. L. Hoard, N. Kim, G. Lang, and C. A. Reed, J. Am. Chem. Soc. **97**, 2676 (1975).
[19]F. Buonocore, F. Trani, D. Ninno, G. Cantele, and G. Iadonisi, Nanotechnology **19**, 025711 (2008).
[20]B. Shan and K. Cho, Phys. Rev. Lett. **94**, 236602 (2005).
[21]C. Rovira, K. Kunc, J. Hutter, P. Ballone, and M. Parrinello, J. Phys. Chem. A **111**, 8914 (1997).
[22]K. M. Vogel, P. M. Kozlowski, M. Z. Zgierski, and T. G. Spiro, J. Am. Chem. Soc. **121**, 9915 (1999).
[23]G. F. Wang, N. Ramesh, A. Hsu, D. Chu, and R. Chen, Mol. Simul. **34**, 1051 (2008).
[24]S. Sun, N. Jiang, and D. Xia, Phys. Chem. C **115**, 9511 (2011).
[25]M. W. Urban, K. Nakamoto, and F. Basolo, Inorg. Chem. **21**, 3406 (1982).
[26]L. M. Proniewicz, I. R. Peng, and K. Nakamoto, J. Am. Chem. Soc. **113**, 3294 (1991).
[27]M. Kozuka and K. Nakamoto, J. Am. Chem. Soc. **103**, 2162 (1981).